Elastomers and Composites
Vol. 47, No. 4, pp. 297~309 (December 2012)
doi: http://dx.doi.org/10.7473/EC.2012.47.4.297

Foaming Behavior, Structure, and Properties of Rubber Nanocomposites Foams Reinforced with Zinc Methacrylate

U. Basuli*, G.-B. Lee*,**, S. Y. Jang**, J. Oh*, J. H. Lee*, S. C. Kim***,
N. D. Jeon***, Y. I. Huh****, and C. Nah*,**,†

**Energy Harvesting WCU Research Team,*
***BIN Fusion Research Team, Department of Polymer-Nano Science and Technology, Chonbuk National University, Jeonju 561-756, Republic of Korea*
****TaeSung Polytec Co., Ltd., Iksan 570-823, Republic of Korea*
*****Department of Polymer and Fiber System Engineering, Chonnam National University, Kwangju 500-757, Republic of Korea*
(Received August 20, 2012, Revised September 7, 2012, Accepted September 17, 2012)

아연 메타아크릴레이트로 보강된 발포고무 나노복합체의 발포거동, 구조 및 특성

운팔 바술리* · 이기쁨*,** · 장세영** · 오재호* · 이지홍* ·
김성철*** · 전남덕*** · 허양일**** · 나창운*,**,†

*전북대 WCU 연구팀, **전북대 BK-21 연구팀, ***태성포리택, ****전남대 고분자섬유시스템공학과
접수일(2012년 8월 20일), 수정일(2012년 9월 7일), 게재확정일(2012년 9월 17일)

ABSTRACT : Different amounts of foaming agents were employed in natural rubber(NR)/butadiene rubber(BR) blends to understand the foaming behavior in presence of nano-reinforcing agent, zinc methacrylate (ZMA). The ZMA greatly improved most of the mechanical properties of the rubber foams, however it did not show considerable effect on the cell morphology, such as cell size, density and porosity. It was also observed that the foaming agent concentration affected all the mechanical parameters. When the content of foaming agent was increased, the number of foams was increased leading to a decrease in density of the compounds. But the size and distribution of foams remained unchanged with increased foaming agent. The effect of high styrene-butadiene rubber (HSBR) was also studied. The size of cells became smaller and the cell uniformity was improved with increasing HSBR. The foam rubber compounds showed much efficient energy absorbing capability at higher strains.

요 약 : 나노보강제의 하나인 아연 메타아크릴레이트 (ZMA)로 보강된 천연고무(NR)/부타디엔고무(BR) 블랜드에 발포제 함량을 달리하여 적용하여 발포거동을 관찰하였다. ZMA 첨가에 따라 전반적인 발포고무의 물성은 향상되었지만, 발포입자크기, 밀도, 발포도 등 발포입자의 모폴로지에는 크게 영향을 미치지 않았다. 발포제의 함량에 따라 발포고무의 기계적 물성은 크게 영향을 받는 것으로 나타났다. 발포제 함량 증가에 따라 발포도가 증가하였고, 이는 발포고무의 밀도감소로 나타났지만, 발포입자의 크기나 분산성은 크게 영향을 받지 않았다. 고함량 스티렌-부타디엔 고무(HSBR)의 영향도 함께 조사하였다. HSBR 함량 증가에 따라 발포입자의 크기는 작아졌고 분산성은 향상되었다. 발포고무는 대변형에서 에너지 흡수성이 뛰어난 것으로 나타났다.

Keywords : foam, zinc metharylate (ZMA), rubber, nano-reinforcing agent, mechanical properties

Ⅰ. Introduction

Because of its extensibility and the ability to spring back, rubber can be selected for foam products and can be freely shaped. Rubber has the advantage of working under dynamic conditions. In recent years, there has been an increasing interest in the preparation and study of rubber foams. However, there is still a lack of information regarding the characterization of foams for structural applications with typical relative densities, that is, the density of the foam divided by that of the respective solid. So, miniaturization and light weight products are possible. Now a day, the focus of the scientific community is the preparing and studying of new rubber-based foams through careful controls on expansion and final cellular

† Corresponding Author. E-mail: *cnah@jbnu.ac.kr*

structure.[1-3] As there are many commercial and industrial applications, foam rubber comes in every imaginable shape and size. Preparation of rubber foam and controlling the shape and size can become very challenging as its structure is very difficult, and remains a problem that has yet to be fully solved. During the last few years, polymer nanocomposite foams have received increasing interest in both the scientific and industrial communities.[4-5] It has been established that small amounts of finely-dispersed nanoparticles may act as sites for bubble nucleation during the foaming process. Particularly, cell density has been starting to increase linearly with clay concentration.[6,7] Moreover, the highest cell density has been obtained when the clay platelets are exfoliated, attaining a higher effective particle concentration and thus higher nucleation efficiency.[6,8] In addition to the higher cell densities, smaller cell sizes have been attained by using nanoparticles. Thus, the presence of exfoliated nanoparticles may result in finer cellular structures due to the combined bubble nucleation and melt strain hardening effects.[9] The nanometric size of the particles also increases the interaction with the polymer matrix, offering a high potential for limited reinforcement, resulting in macroscopic mechanical enhancement. If one considers the micrometer or submicrometer thickness of the cell walls in foams, the very small size of the nanoparticles could act locally to reinforce them. In the case of layer-like nanoparticles, improved barrier properties can also be expected by the nanosized platelets by limiting gas diffusion during the expansion and stabilization of the foam structure.[4]

Reinforced ethylene-propylene-diene terpolymer (EPDM) and nitrile rubber (NBR) blends have been compounded with azodicarbonamide (ADC/K) foaming agent by Lawindy et al.[10] to obtain EPDM/NBR foam composites. It has been observed that the mechanical properties decreased as the foaming agent and/or temperature was increased. The demand for a rubber compound which has a high stability and good durability under heat-aging and chemical substance exposure has progressively increased. In recent years, research on carbon black, silica, clay, and carboxylic acid metallic salt filled polymer nanocomposites has increased.[11-13] Unsaturated carboxylic acid metallic salt, such as zinc methyl acrylic acid (ZMA) typically induce a rigid block of 20~30 nm size by phase separation using crosslink reaction with elastomer, notably polar ones. Through this reaction, elastomer nanocomposite has been made which has a high strength and research of this composite being progressed.[13-17] Commonly, elastomer nanocomposite crosslinked with unsaturated carboxylic acid in the presence of peroxides shows a good tensile strength, tearing strength, wear resistance, extreme condition resistance, hardness, and tensile modulus.[15,17-23] The reinforcing zinc clusters of ~20-30 nm in size are formed by co-polymerization of carboxylate in itself during the crosslink reaction. An ionic bond is formed between elastomer chains by graft reaction, which reinforces the elastomer. A variety of studies on these kinds of composites have been conducted by Lu et al.[17] who concentrated on the reinforcing effect of ZMA in hydrogenated acrylonitrile-butadiene rubber (HNBR). They found that ZMA-filled composites have a higher tensile and tearing strength than the more commonly used carbon black (CB) filled composites. In another study, the effects of metallic acrylate, such as magnesium and zinc, on different types of rubber composites based on natural rubber (NR), butadiene rubber (BR), styrene butadiene rubber (SBR), ethylene-propylene-diene monomer (EPDM), acrylonitrile-butadiene rubber (NBR) and HNBR[17,19-26] were investigated. Concurrently, some ZMA-reinforcing rubber compounds have been developed for industrial applications due to the excellent overall properties of ZMA/rubber vulcanizates.[27-30] The Properties of foam rubber are influenced by properties of rubber, foam density, size and number of cells, and distribution of cell structure.[31-33] It has also been observed that foam density is influenced by a variety of parameters, such as rubber type, concentration of crosslinks and foaming agent, and the technical processing and conditions.[34-37]

Polyurethanes (PUs) are unique polymer materials with a wide range of physical and chemical properties. Due to their high-energy absorption capabilities, PU foams have been widely used in many applications, such as, a bumper stopper provided in the vicinity of a piston rod in a shock absorber to elastically limit the stroke. It absorbs the shock generated by the stroke at the time of the contraction. The mechanical behavior of PU foams has been attracting attention from engineers and researchers. PU foam can be either closed or open cell, and can absorb energy by undergoing a large-scale compressive deformation. It has been observed that both tensile and compressive strains are developed inside the foam specimens due to the inhomogeneous deformation of the foam specimens during compression and that there is a large tensile strain concentration at the interface of the foam specimen and the protected object. The tensile deformation can cause failure of the foam specimen through crack propagation.[38,39] Very recently, flexible polyurethane foams were also prepared by Kang et al.[40] The rubbery properties of polyurethane foams mainly depend on the crosslink density of the polyurethane. However, PUs also have some disadvantages, such as low thermal stability and problems with long-term mechanical strength resistance due to inevitable hydration, etc. To overcome these disadvantages, a great deal of effort has been devoted to the development of nanostructure polyurethane composites in recent years.[41-45]

In this study, a new type of rubber nanocomposite foam has been prepared by mixing various amounts of ZMA, NR and BR blends through two types of foaming process operations. Both NR and NBR rubber blends were compounded

with different concentrations of CB and ZMA. The mechanical parameters in both extension and compression, such as modulus of elasticity (E), tensile strength, strain-to-break, and degree of compressibility are calculated. The effect of high styrene-butadiene rubber (HSBR) on foam properties has been compared by cell size, morphology, and physical properties. Furthermore, the physical properties of the foams, in terms of their tensile strength, elongation-at-break, tear strength, and hardness were investigated as a function of the reinforcing filler concentration.

Ⅱ. Experiment

1. Materials

In this study, commercial grade natural rubber (NR, RSS# 3, Thailand) and polybutadiene (BR, KBR-01, Kumho Petrochemical Co., Korea) were used as the base materials. Semi reinforcing furnace black, SRF (N774) (Evonik Carbon Black, Seoul, Korea Co.) and zinc methacrylate (ZMA) (Sigma-Aldrich Chemical Co., USA) were used as fillers. High styrene-butadiene rubber (HSBR, bound styrene content: 68wt%, Kumho Petrochemical Co., Korea) was used as reinforcement material. Compounding and curing additives such as ZnO (Hanil zinc), stearic acid (LG chemical, Korea), and dicumyl peroxide (DCP) (Aldrich Chemicla Co., USA) were used as crosslink agents. Other ingredients, such as antioxidants (3C, RD, P-wax), blowing agent (DW150), processing aid (EXTON K-1), flow enhancer (A#2 oil), lubricating and moisture protection (WD) and peptizer (P-3S) were purchased from local suppliers (analytical grade). A chemical foaming agent of p-oxybis-benzene-sulfonylhydrazide (OBSH, OHW2, decomposition temperature of 160 ± 3 ℃, Dongjin Co.) was used.

2. Compounding

Initially, rubbers (NR, BR and HSBR) were mixed in a Banbury mixer at 140 ℃ for 30 s with a rotor speed of 60 rpm using a fill factor of 75%. The reinforcing agents and activator were then added onto the rubber and mixed for another 180 s. Next, the other ingredients (CB, ZMA, processing oil, cure activators) were mixed for 210 s. The final batch was made by a two roll-mill (Farrel 8422, USA) after 24 hours from finishing time of master-batch preparation at a rotation speed of 15.3 rpm at around 90 ℃ for 10 minutes. After 24 hours optimum crosslink time was measured using a rheometer (ODR, Alpha Technologies, USA). The formulations and designations of all the rubber composites are shown in Table 1. Foam was made using two methods: the first method was a single step process, as shown in scheme 1 (a), while the other is a two-step process, as shown in scheme 1 (b). The mold was filled to 83% of the optimum volume of the mold to provide enough space for foam cell formation. Foam containing HSBR was made in two steps. The first step was the production of pre-foam at 100 ℃ for 10 minutes by using a pre-formed mold. The second step included crosslinking and foaming at 160 ℃ for optimum crosslink time. Sample designations are given according to the following: Ra/b/c/d, where

Table 1. Formulations of NR/BR Foam Composites (unit: phr)

Compounds #	R6/4/4/0	R6/4/4/4	R6/4/4/8	R6/4/5/0	R6/4/5/4	R6/4/5/8	R6/4/6/0	R6/4/6/4	R6/4/6/8	R5.5/3.5/5/4	R5.5/3.5/5/8	R5/3/5/4	R5/3/5/8
NR	60	60	60	60	60	60	60	60	60	55	55	50	50
BR	40	40	40	40	40	40	40	40	40	35	35	30	30
HSBR	-	-	-	-	-	-	-	-	-	10	10	20	20
ZnO	5	5	5	5	5	5	5	5	5	5	5	5	5
S/A	1	1	1	1	1	1	1	1	1	1	1	1	1
CB	40	40	40	40	40	40	40	40	40	40	40	40	40
ZMA	40	40	40	50	50	50	60	60	60	50	50	50	50
RD	2	2	2	2	2	2	2	2	2	2	2	2	2
DW150	2	2	2	2	2	2	2	2	2	2	2	2	2
DCP	1	1	1	1	1	1	1	1	1	1	1	1	1
OHW2	0	4	8	0	4	8	0	4	8	4	8	4	8

S/A = Stearic acid, RD = Antioxident, DW150 = Blowing agent, OHW2 = Chemical foaming agent.
*Sample designations are given according to the following: Ra/b/c/d where R=Rubber composites, a/b/c represents NR/BR/ZMA weight ratio and d represent amount of OHW2 (phr).

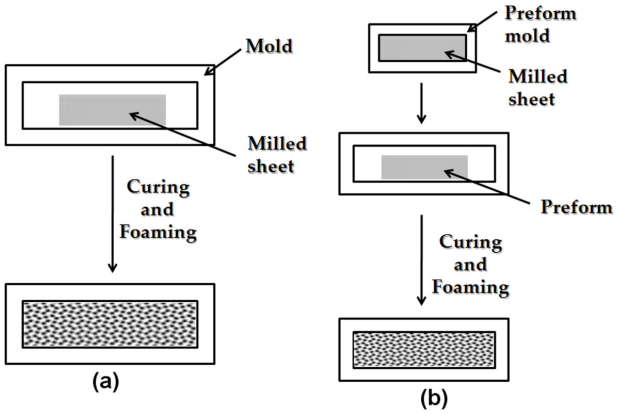

Scheme 1. Foaming process of rubber compounds: (a) Single stage process and (b) Two stage process.

R=Rubber composites, a/b/c represents NR/BR/ZMA weight ratio, and d represents the amount of OHW2 (phr).

3. Testing and Characterization

3.1 Rheometer

Curing characteristics of the composites were determined using an Oscillating Disc Rheometer (ODR, Alpha Technologies, USA) at 160 ℃ (Figure 2). The vulcanization characteristics of maximum torque (M_H), minimum torque (M_L), scorch time (ts_2) and optimum curing time (t_{90}) were performed. Tests were obtained in accordance with ASTM D2084 and the error in measurement of the torque was limited to ±5%.

3.2 Thermal gravimetry analysis (TGA)

Non-isothermal TGA measurements were performed with 10-12 mg of samples using a Perkin - Elmer Thermal Analysis Instrument, USA, under a nitrogen atmosphere (flow rate of 60 ml/min) from 30 °C to 800 °C, and operated at a heating rate of 10 °C /min. Isothermal tests were also carried out in a nitrogen atmosphere at 160 °C for 60 min using the same TGA instrument as depicted earlier. Prior to isothermal heating, the sample was heated at a rate of 30 °C/min from the ambient temperature to the selected temperature for isothermal degradation. As soon as the system reached the selected temperature, the variation of sample mass with time was recorded. The error in measurement of temperature was within ± 0.05%.

3.3 Morphological analysis

To check cell size, structure, and orientation, the morphology of foam rubber composites was measured using scanning electron microscopy (SEM), as well as an optical microscope, after the cutting of the sample using a razor, and then coating the cut surfaces with gold. The sample surface was sputter coated with a thin gold layer (3.0 nm thickness) and then examined under the JEOL JSM 5900 digital scanning electron microscope (Japan). The images were obtained at a tilt angle of 0°, with an operating voltage of 20 kV and average beam current of 90 mA. The average size and number of cells were calculated in a unit area.

3.4 Foam property

Density of foam was calculated using a sample cut to a circular shape 20 mm in diameter. After measuring the weight it was then converted into weight per unit volume (g/cm^3). The voids-volume was calculated using equation (1). The rate of foaming was estimated by calculating the porosity rate given by equation (2).

$$Volume\,of\,voids\,(V_v) = \frac{4\pi r^3}{3} \times n \quad (1)$$

$$Porosity\,rate\,(\%) = \frac{Volume\,of\,voids\,(V_v)}{Total\,volume\,(V_t)} \times 100 \quad (2)$$

where r and n are average radius and number of cells, respectively. V_t is total volume and V_v is volume of foaming cell. Average size of cell was calculated based on SEM image analysis and calculations.

3.5 Hardness

The hardness of all the samples was measured with a durometer (Shore A type) according to the procedure described in ASTM D 2240-97, at room temperature. The average thickness and diameter of the hardness specimen is about 6 mm and 10 mm, respectively. For each sample, the average of ten tests is reported here. The percentage error associated with the hardness measurements were within ±2%.

3.6 Tensile property

Tensile tests were carried out according to ASTM D 412-98 with dumbbell-shaped specimens using a tensile tester (LLOYD Instrument, UK) in uniaxial tension mode at a constant crosshead speed of 500 mm/min. The tests were performed at ~30 °C. For each sample, the averages of five tests were reported here. From the stress-strain curve, tensile strength, elongation at breaking and modulus were obtained. In each case, the errors corresponding to tensile modulus and tensile strength measurement were limited to ±1% and ±2%, respectively.

3.7 Tearing property

Tearing strength was measured using a trouser specimen. Trouser specimens of length 95 mm, width 35 mm and thickness ~ 0.85 mm, with a precut of 20 mm at the center that was used for the tear energy measurement (fracture energy or strain energy release rate) of the vulcanizates. The speci-

mens were tested at a constant crosshead speed of 50 mm/min. To minimize the extension of the legs of the trouser specimens during measurement, cotton cloth was attached to both sides of the sample. Cotton cloth of 10 mm wide was placed along both sides of the test specimens and thus the effective unreinforced width was 15 mm. In this arrangement of the trouser test, the tear energy is given by the following relationship.

$$G_c = \frac{2(\alpha_s)^2 F}{d} \quad (3)$$

where F is the force applied to the end of the test piece, α_s is the swelling ratio and d is the thickness of the torn path. Tearing energy G_c was calculated by using equation (3) with the measured tearing strength F.

3.8 Compressive strength property

Compression testing was carried out using a LLOYD Instrument, UK. The sample was made by secondary pressure process and the shape was a bellow-shaped trapezoid cylinder with height, diameter of the base side, and diameter of the upper side of 100 mm, 55 mm, and 40 mm, respectively. Compressive strength was measured under a 16 kN limiting load after three preliminary compressive tests, with 50 mm/min of constant compressive speed, and 5 kN of limiting load at room temperature.

Ⅲ. Results and Discussion

1. Thermogravimetric Analysis (TGA) Studies

Thermo gravimetric analysis (TGA) is an excellent tool for studying the kinetics of thermal degradation of any organic sample. An optimum decomposition temperature of OHW2 was confirmed by TGA thermogram analysis. The representative TGA thermogram of the OHW2 sample is shown in Figure 1 (a-b). The TGA curves of OHW2 show that the major decomposition region is centered between 150 °C and 170 °C. From Figure 1 (a), it is confirmed that no weight loss of OHW2 occurred before 150±3 °C. OHW2 starts to degrade in a nitrogen atmosphere at about 155 °C up to 166 °C. Sharp weight loss (about 60%) occurs at about 160 °C. Thus, 160±3 °C is considered as the foaming start temperature.

Figure 1 (b) shows the weight loss of OHW2 with time at 160 °C (foaming start temperature). OHW2 exhibits a more rapid degradation under isothermal heating at temperatures higher than 160 °C. The single-step weight loss and drastic degradation of OHW2 have been observed during the first few seconds of isothermal decomposition, followed by no weight loss within this period (60 min). So, it seems that the crosslink reaction occurs after foaming of the foam cell.

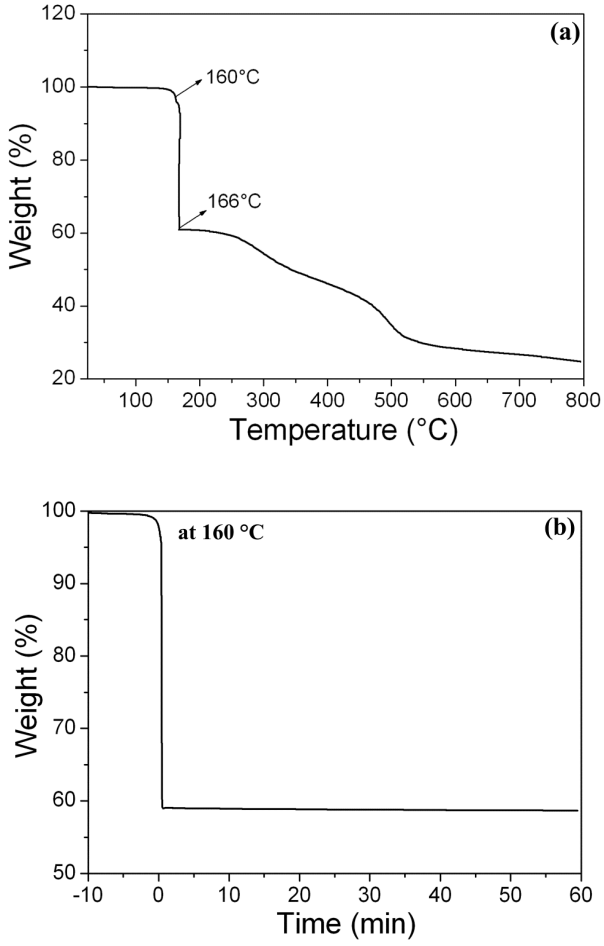

Figure 1. TGA thermogram of OHW2 sample: (a) Non-isothermal and (b) Isothermal at 160 °C.

2. Effect of ZMA

2.1 Curing characteristics

The optimal crosslinking condition is a critical requirement for optimizing foam expansion and ensuring good physical properties for the foams. The curing characteristics of the foamed compounds at 160 °C with different filler contents are presented in Figure 2. The cure characteristics were studied for different CB/ZMA contents. The variation of torque values with crosslink time are shown in Figure 2. It has been observed that the torque increased linearly with the increase of ZMA content. This may be due to the generation of free radicals formed by the chemical reaction between ZMA and DCP. These free radicals are combined to form chemical grafts to the rubber backbone chains and the cluster formations of dangling zinc ions. The physical crosslinks of ion clusters also give rise to the higher crosslinking density. However, the rate of cure reaction was delayed somewhat with increasing ZMA content. It has also been observed that the torque of rubber

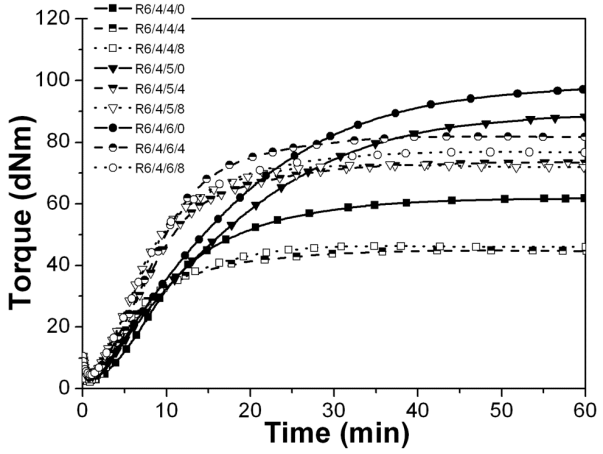

Figure 2. The cure characteristics of the various foamed compounds at 160 °C.

compounds that do not contain foaming agent are higher than the compounds that do contain foaming agent. In the case of R6/4/4/0, which does not contain OHW2, the cure torque is almost unchanged after 20 min. On the other hand, the torque of all compounds increased linearly with increasing ZMA content. But the cure torque decreased with the increase of OHW2 content. This may be due to the generation of free radicals formed by the chemical reaction between ZMA and DCP. The highest torque is shown at higher concentrations of ZMA and when using dual reinforcement composites, when compared to the other systems. This may increase the total crosslink density in the rubber composites and aid formation of ionic clusters. According to previous studies, the rubber composite was reinforced by metallic acrylates due to physical adsorption, chemical grafting and ionic cluster structure formation.[46,47]

2.2 Foam microstructure and morphology

Foam compounds containing various amounts of ZMA and foaming agents were analyzed using SEM. Figure 3 (a-f) represents the typical microstructures of R6/4/4/4, R6/4/48, R6/4/5/4, R6/4/5/8, R6/4/6/4, and R6/4/6/8, respectively. For all composites, the foaming cells are closed and cell size is not affected by the degree of crosslink. This indicates that crosslinking occurs after formation of the foaming cell by release of gases at the initial stage of the crosslinking reaction. It is also observed that the number of such cells increases with the increasing amount of foaming agent. The effects of foaming agent content on the foaming characteristics were studied by investigating the apparent densities and porosity ratios of the foam at different filler contents. The average cell size, numbers of such cells in rubber foams, average porosity rate, and density are calculated, and the results are plotted in Figures 4-5. The average cell size is measured from SEM photomicrography, and is shown in Figure 3. As expected, the density (g/cm^3) and the porosity rate show an opposite trend to each other. It should be noted here that both the density and rate of porosity are not greatly affected by either the crosslink density or the ZMA content. On the other hand, if the amount of foaming agent was increased, the rate of porosity increased but density decreased. In the case of R6/4/6/8, both

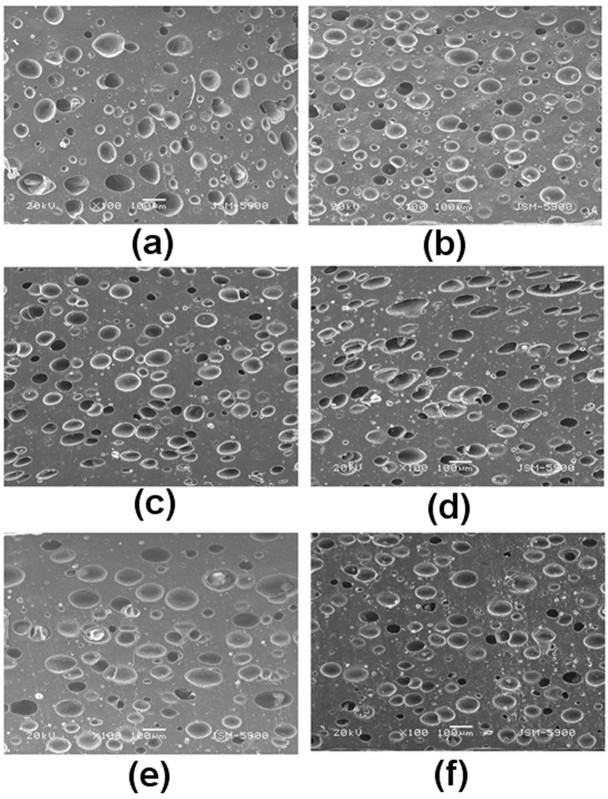

Figure 3. SEM photo micrographs of razor cut surfaces of microcellular rubber foams (100 x magnification): (a) R6/4/4/4, (b) R6/4/4/8, (c) R6/4/5/4, (d) R6/4/5/8, (e) R6/4/6/4 and (f) R6/4/6/8, respectively.

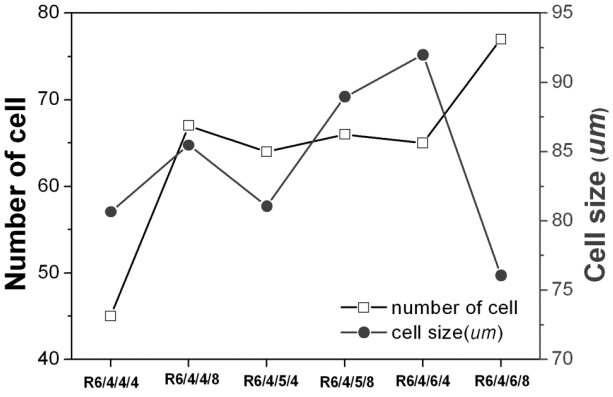

Figure 4. Average cell size and the number of such cells of various foams composites.

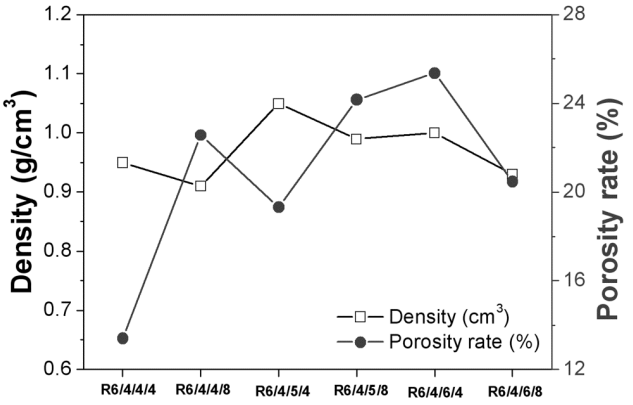

Figure 5. Density and porosity ratio of various rubber foams.

the density and porosity rate decreased with an increase of foaming agent. This may be due to the formation of a large number of small sized cells throughout the matrix (Figure 3f). As shown in Figure 5, the foam density increased with increasing ZMA content (foaming efficiency decreased), while it decreased with foaming agent content. It is common that the density increases with increasing filler content because of the higher density of filler. However, in this case, no significant increase of density with increased ZMA content has been observed. Low densities of foams are indicating a better blowing efficiency. Compounds possessing the lowest blowing efficiency and highest density, exhibit better tensile properties. It has also been observed that more uniform foaming cells can be obtained from ZMA filled composites. It seems that low density foam results from a smaller cell size with an increase of foaming agent.

2.3 Hardness

Hardness values of foamed rubber compounds are also found to be a function of both the concentration of foaming agents and ZMA loading, as shown in Figure 6. As expected, the hardness of foamed compounds was lower than normal and it decreased with the increasing amount of foaming agent. However, only a small increase in the hardness values could be observed. The hardness increased sharply with increasing ZMA content up to 50 phr, and then increased only slightly upon further loading. For 40 phr ZMA-filled composites, the hardness decreased drastically with increasing foaming agent, whereas for other composites, hardness decreased to some extent with increasing concentration of foaming agent. One of the most interesting observations about hardness of R6/4/5/4 and R6/4/6/4 is that at 4 phr OHW2 loading, the R6/4/5/4 shows higher hardness values than R6/4/6/4. This may be due to the formation of a small number of small cell sized foams in R6/4/5/4. On the other hand, in R6/4/6/4 cell size and numbers of such cells are greater than R6/4/5/4. At high OHW2 loading (8 phr) the differences in hardness between the two compounds R6/4/5/8 and R6/4/6/8 are not very significant. This may be due to the combined effect of the ZMA and foaming agent and can be attributed to the hardness of ZMA and foaming efficiency.

2.4 Tensile property

Representative stress-strain curves of all composites are depicted in Figure 7. All the composites show a similar pattern for the stress-strain curves. Normal rubber compounds (without foaming agent) show a high tensile strength, elongation at breaking, and modulus at 100% elongation (Figure 8). The change in the elongation at break of all the foamed compounds is shown in Figure 7. The elongation at break decreases continuously when increasing the filler loading. Foam rubber compounds show comparatively lower tensile properties than normal compounds, but these compounds show a similar pattern to the normal rubber compound in stress-strain behavior. The tensile strengths increased steadily with increasing ZMA content because of the reinforcing effect of ZMA. Comparison

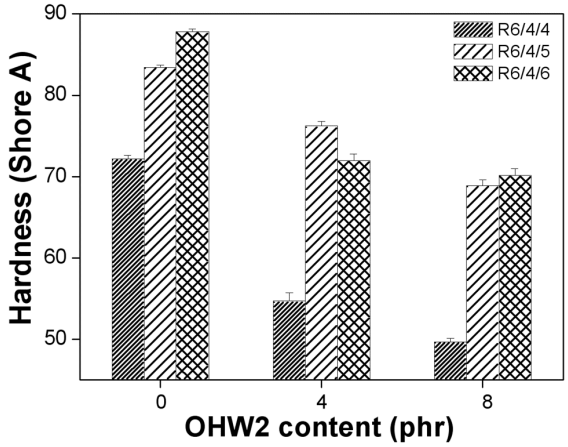

Figure 6. Variation of the hardness as a function of ZMA and foaming agent content.

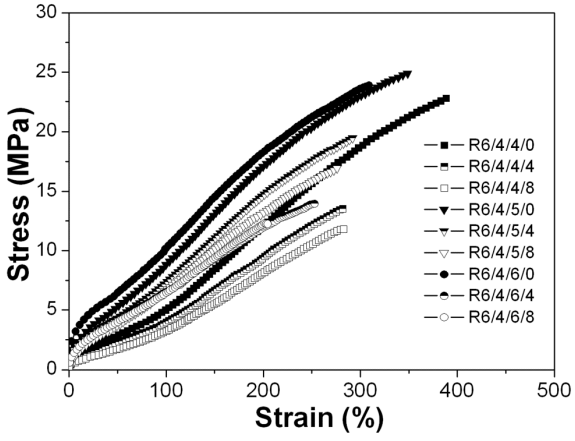

Figure 7. Stress-strain plot of various nanocomposites foam.

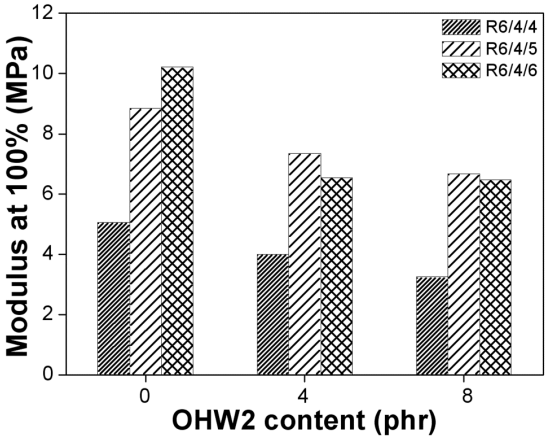

Figure 8. Tensile modulus at 100% elongation with foaming agent content.

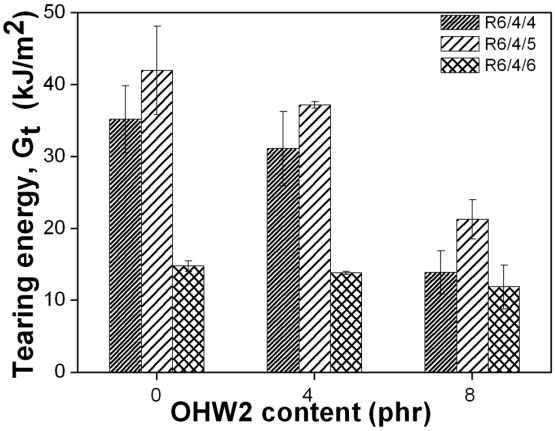

Figure 9. Variation of tearing energy values with foaming agent content.

all the tensile properties of R6/4/5/0 compound shows that it is better than the R6/4/6/0 compound. Generally, highly-crosslinked polymers have improved physical properties when compared to others, but in the case of foam compounds, the physical properties improve with an increase of density. In this study, R6/4/5/4, which has foaming agent, shows a higher tensile strength and modulus at 100% elongation than R6/4/4/0, with no foaming agent. This may be due to the high filler loading and interaction between the filler and rubber matrix, leading to formation of a strong foaming cell. This may also be due to the optimum volume fraction of ZMA acting as a reinforcing filler for the rubber matrix. In other words, the volume fraction of ZMA will be increased upon increasing the ZMA loading, so the reinforcement of the rubber matrix will be effective for making the samples stronger. At higher loading cases, such as 60 phr of ZMA, the dispersion of ZMA particles is not uniform. The ZMA particles directly involved in the cross-linking bond were useful for increasing the initial modulus values. Some ZMAs are not able to form crosslinks with rubber chains because the organic chains of ZMA are too short. However, they can form ionic clusters through static electronic attraction.[48]

2.5 Tear property

Tear strength (G_c) was measured using the trouser test as shown in Figure 9. Unlike tensile strength, the tear strength of R6/4/5/0 rubber compounds are higher than R6/4/6/0. This may again be due to the result of poor dispersion of ZMA in the rubber matrix. At a high filler concentration the dispersion of ZMA is not good enough to give rise to an effective reinforcement.[19,49] The crosslink reaction occurs through the aggregated ZMA particle and the aggregated ZMA particle may act as a plasticizer. The tear strength of foam compound was lower than that for normal compounds and decreased with the increasing foaming agent content. In an attempt to check

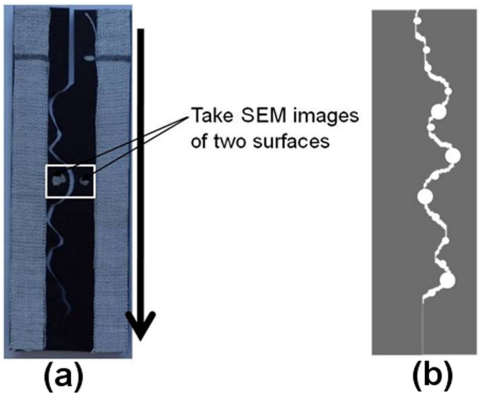

Scheme 2. Examination of crack surfaces: (a) Portion of crack in trouser test samples from which SEM image has taken and (b) Hypothesis of failure following by cavity formation.

the effect of the foaming cell on the physical property of foam compounds, both sides of the torn areas of the sample, as Scheme 2 (a) were observed by SEM. The representative SEM photo micrographs are presented in Figure 10. The tearing occurred along the foam cells as shown schematically in Scheme 2 (b).

3. Effect of HSBR

3.1 Foaming property

The cut surfaces of foam compounds employed by a small amount of high styrene SBR (HSBR) and foaming agent were observed by optical microscope, and are presented in Figure 11. In order to check the foaming efficiency, the cell size and average number of such cells have been measured and these results are shown in Figure 12 (a-b). All foaming cells were closed and of greater size than foaming cells produced by the one-step foaming process. The size of foaming cell decreased,

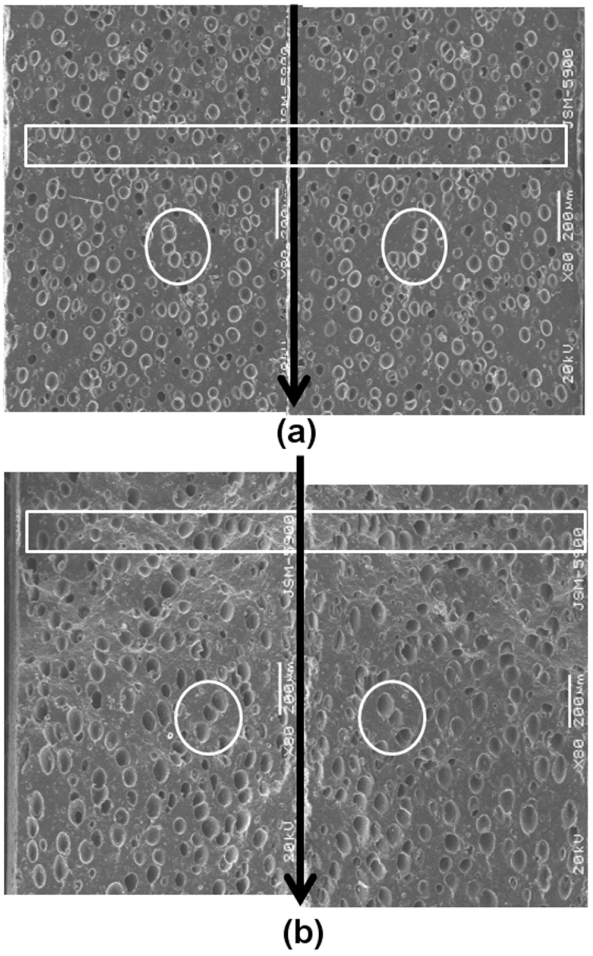

Figure 10. Representative SEM photomicrographs of both side of crack area of samples:
(a) Two surfaces of R6/4/4//8 trouser sample and (b) Two surfaces of R6/4/6/8 trouser sample.

while the number of cells increased with the increase of foaming agent content. When the HSBR was added, the foaming cell was more uniform, but the size was reduced. The addition of HSBR makes the formation of foaming cells easier. With the increase of foaming agent loading, a larger number of uniform foaming cells were formed, but this foaming behavior did not affect the physical property deterioration.

3.2 Hardness

The variation of hardness properties with HSBR content is shown in Figure 13. Hardness increased with an increase of HSBR content, whereas it decreased with increasing foaming agent content. This may be due to the decreasing density of the foam.

3.3 Tensile property

Representative tensile stress-strain curves for different rubber compounds containing HSBR are presented in Figure 14.

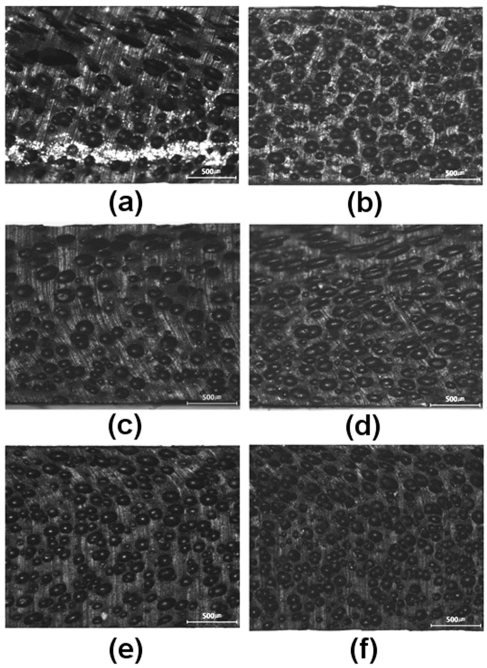

Figure 11. Representative polarization microscope images (X5) of various rubber foam compounded with HSBR: (a) R6/4/5/4 (b) R6/4/5/8 (c) R5.5/3.5/5/4 (d) R5.5/3.5/5/8 (e) R/5/3/5/4 and (f) R/5/3/5/8.

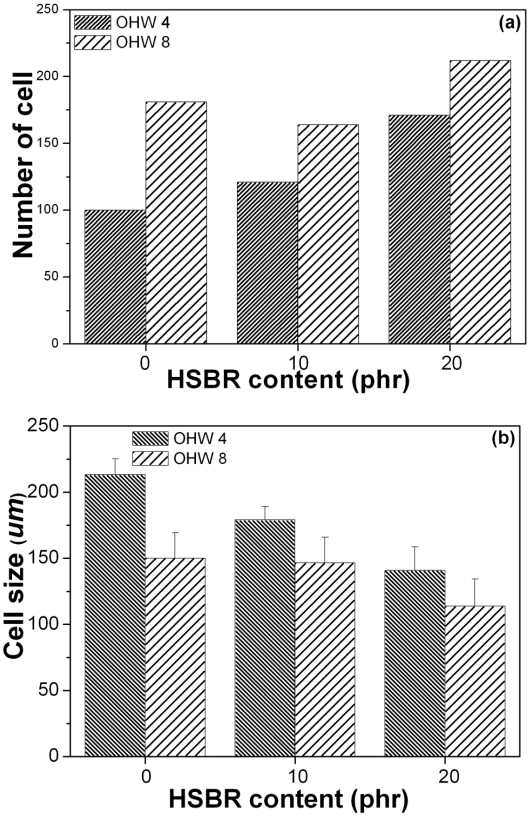

Figure 12. Variation of rubber foams properties with HSBR content: (a) The number of cell and (b) Average cell size.

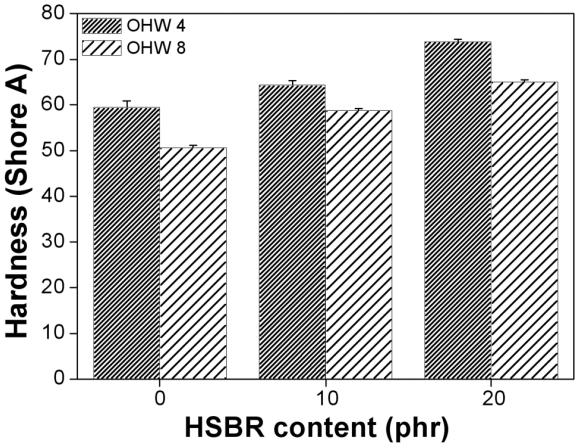

Figure 13. Variation of hardness with HSBR content.

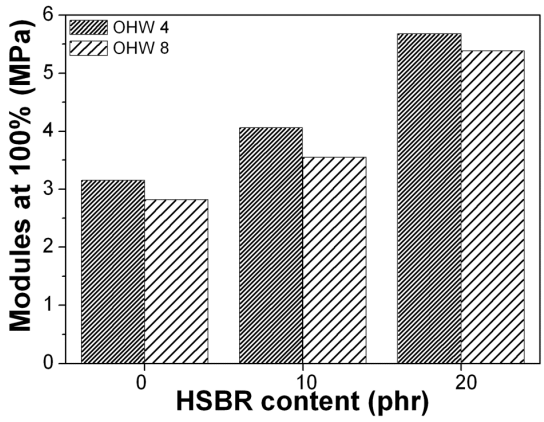

Figure 15. Variation of modulus at 100% elongation with HSBR content.

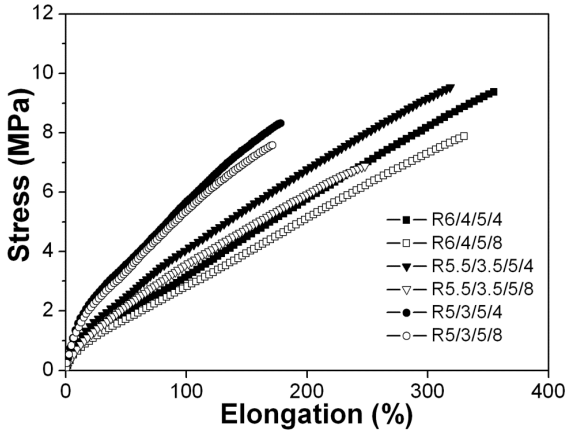

Figure 14. Tensile behavior of various rubber foam containing HSBR.

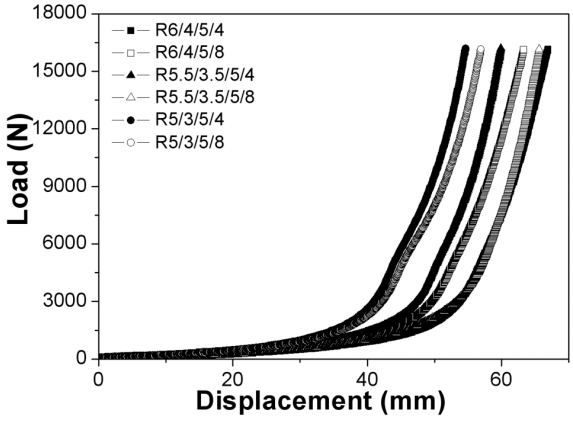

Figure 16. The load versus deflection curves (compression property) of various rubber foams.

The figure well illustrates that for all specimens the stress increases slowly and linearly with the rising tensile strain. Tensile data modulus at 100% elongation is plotted against HSBR content in Figure 15. Tensile strength, elongation at breaking, and 100% modulus decreased with an increase of foaming agent content. With increasing concentrations of HSBR, the tensile strength of the foam compounds increased initially, then reached a maximum at a particular concentration (10 phr), then decreased. A similar trend is observed for modulus values at higher elongations. Elongation-at-break was found to be diminished with the increase in HSBR content. The possible reason for having a maximum tensile strength and high elongation at break, at 10 phr HSBR loading (R5.5/3.5/5/4 and R5.5/3.5/5/8) is due to having a favorable cell size and number of such cells per unit area. At 20 phr of HSBR loading (R5/3/5/4 and R5/3/5/4) composites show high tensile properties. Generally, in foam compounds, the density and physical properties are interrelated. However, tensile property decreases with increasing OHW2 content. The low tensile property is the result of a decreased foam density with increasing foaming agent content.

3.4 Compressive strain property

The load-compression behavior of foam reflects its geometric structure and the physical properties of the matrix polymer. Therefore, it is very important to understand the compressive strain behavior of the foam specimens, notably for applications like bumper stoppers in cars to effectively absorb strong shocks from the roads.[50] Experimental data obtained in this study was compared with data from the conventional flexible polyurethane foams. Compression testing has been conducted to study the inhomogeneous deformation of the foam specimens and there are large tensile strain concentrations at the interfaces of the foam specimen and the protected object. The load versus deflection curves are shown in Figure 16. In the early stage, all foam compounds exhibited a big change, after that the degree of change decreased and compressive strength increased sharply. In these early stages,

change occurred easily with very little energy because the change depended on the wall of foaming cell. However, after compression of a cell, the physical property of the normal compound is reflected. R5/3/5/4 and R5/3/5/8, having higher concentrations of HSBR, show the lowest change, with the degree of change increasing with the increase of foaming agent content. But R6/4/5/4 show similar deformation actions when compared with R5.5/3.5/5/8. Using these established relationships, it is now possible to precisely explain the structural features a foam must possess in terms of density, cell shape and size distribution, and modulus of the base polymer, to meet a given load-compression specification. There has been considerable increase in interest the use of foams for lightweight structural machinery and energy absorption parts, such as in the automobile, railway and aerospace industries, for they have a wide plateau in the compressive stress-strain curve.[51-53] In our case 50 phr ZMA (R6/4/5/4 and R6/4/5/8) and R5.5/3.5/5/8 show wide ranging plateaus.

Ⅳ. Conclusions

Reinforced NR/BR foams have been successfully prepared using a compression molding method. The tensile strength of the foam compounds increased with increasing filler content because of the reinforcing effect. Furthermore, the tensile strength modulus of the samples increased continuously with ZMA content, and decreased with increasing foaming agent. Foaming properties, such as cell size and number of cells, were not affected much by ZMA content. The elongation at break dropped continuously with increasing foaming agent and ZMA content. At 50 phr, ZMA loading nanocomposites foam showed a higher cell density with a smaller cell size. It has also been observed that the amount of foaming agent has a significant effect on the physical properties of foam. The effect of HSBR on the properties of this foam compound has also been studied. The tensile moduli of the composites increased significantly with the incorporation of HSBR, particularly at higher concentrations. With increasing HSBR and blowing agent content the cells became smaller and more uniform. R5.5/3.5/5/8 form compound showed a high harness and more uniform foaming cell size. Composites (R6/4/5/4 and R5.5/3.5/5/8) have a wide plateau in their compressive stress-strain curves. The cellular structure prepared in this process has been shown to have a significant effect on the corresponding tensile property of foams. It shows that the foam can absorb more energy at high strain rates and is very useful in shock protection.

Acknowledgments

This research was carried out under the Industry Fusion Core Technology Development Program of the Ministry of Knowledge Economy and by Taesung Polytec Company of small business innovation development program.

References

1. M. A. Rodríguez-Pérez, "Crosslinked polyolefin foams: production, structure, properties, and applications", *Adv. Polym. Sci*., **184**, 97 (2005).
2. J. I. Velasco, M. Antunes, O. Ayyad, J. M. López-Cuesta, P. Gaudon, C. Saiz-Arroyo, M. A. Rodríguez-Pérez, and J. A. de Saja, "Foaming behaviour and cellular structure of LDPE/hectorite nanocomposites", *Polymer*, **48**, 2098 (2007).
3. M. Antunes, V. Realinho, and J. I. Velasco, "Foaming Behaviour, Structure, and Properties of Polypropylene Nanocomposites Foams", *J. Nanomater*., doi:10.1155/2010/306384 (2010).
4. L. J. Lee, C. Zeng, X. Cao, X. Han, J. Shen, and G. Xu, "Polymer nanocomposite foams", *Compos. Sci. Technol*., **65**, 2344 (2005).
5. M. Antunes, V. Realinho, and J. I. Velasco, "Foaming Behaviour, Structure, and Properties of Polypropylene Nanocomposites Foams", *J. Nanomater*., **2010**, 1 (2010).
6. C. Zeng, X. Han, L. J. Lee, K. W. Koelling, and D. L. Tomasko, "Polymer-clay nanocomposite foams prepared using carbon dioxide", *Adv. Mater*., **15**, 1743 (2003).
7. Y. Di, S. Iannace, E. Di Maio, and L. Nicolais, " Poly(lactic acid)/organoclay nanocomposites: thermal, rheological properties and foam processing", *J. Polym. Sci. B*, **43**, 689 (2005).
8. X. Han, C. Zeng, L. J. Lee, K. W. Koelling, and D. L. Tomasko, "Extrusion of polystyrene nanocomposite foams with supercritical CO_2", *Polym. Eng. Sci*., **43**, 1261 (2003).
9. M. Okamoto, P. H. Nam, P. Maiti, T. Kotaka, T. Nakayama, M. Takada, M. Ohshima, A. Usuki, N. Hasegawa, and H. Okamoto, "Biaxial flowinduced alignment of silicate layers in polypropylene/clay nanocomposite foam", *Nano Lett*., **1**, 503 (2001).
10. A. E. Lawindy, K. M. A. El-Kade, W. E. Mahmoud, and H. H. Hassan, "Physical studies of foamed reinforced rubber composites Part I. Mechanical properties of foamed ethylene propylene-diene terpolymer and nitrile-butadiene rubber composites", *Polym. Int*., **51**, 601 (2002).
11. H. M. Da Costa, L. L. Y. Visconte, R. C. R. Nunes, and C. R. G. Furtado, "Use of Rice Husk Ash as Filler in Natural Rubber Vulcanizate: In comparison with Other Commercial Fillers", *J. Appl. Polym. Sci*., **83**, 2331 (2002).
12. P. L. The, Z. A. Mohd Ishak, A. S. Hashim, J. Karger-Kocsis, and U. S. Ishiaku, "On the potential of organoclay with respect to conventional fillers (carbon black, silica) for epoxidized natural rubber compatibilized natural rubber vulcanizates", *J. Appl. Polym. Sci*., **94**, 2438 (2004).
13. N. Nagata, T. Sato, T. Fujii, and Y. Saito, "Structure and mechanical properties of hydrogenated NBR/zinc dimethacry-

late vulcanizates", *J. Appl. Polym. Sci. symp*., **53**, 103 (1994).
14. Y. Lu, L. Liu, C. Yang, M. Tian, and L. Zhang, "The morphology of zinc dimethacrylate reinforced elastomers investigated by SEM and TEM", *Eur. Polym. J*., **41**, 577 (2005).
15. J. W. Lee, H. S. Joo, S. C. Kang, and Y. W. Chang, "Effect of zinc dimethacrylate on mechanical properties of dynamically vulcanized polypropylene(PP) and nitrile rubber(NBR) blends", *Elastomer*, **41**, 245 (2006).
16. Y. Lu, L. Liu, D. Shen, C. Yang, and L. Zhang, "Infrared study on *in situ* polymerization of zinc dimethacrylate in poly (α-octylene-*co*-ethylene) elastomer", *Polym. Int*., **53**, 802 (2004).
17. Y. Lu, L. Liu, M. Tian, H. Geng, and L. Zhang, "Study on mechanical properties of elastomers reinforced by zinc dimethacrylate", *Eur. Polym. J*., **41**, 589 (2005).
18. A. Du, Z. Peng, Y. Zhang, and Y. Zhang, " Polymerization conversion and structure of magnesium methacrylate in ethylene-vinyl acetate rubber vulcanizates", *J. Appl. Polym. Sci*., **93**, 2379 (2004).
19. W. S. Jin, H. S. Lee, and C. Nah, "Preparation and physical properties of acrylonitrile-butadiene rubber nanocomposites filled with zinc dimethacrylate", *Polymer* (*Korea*), **28**, 185 (2004).
20. J. H. Won, H. S. Joo, and Y. W. Chang, "Preparation and Properties of EPDM/Zinc Methacrylate Hybrid Composites", *Elastomer*, **40**, 59 (2005).
21. Z. Peng, X. Liang, Y. Zhang and Y. Zhang, "Reinforcement of EPDM by *in situ* prepared zinc dimethacrylate", *J. Appl. Polym. Sci*., **84**, 1339 (2002).
22. X. Yuan, Z. Peng, Y. Zhang, and Y. Zhang, "*In situ* preparation of zinc salts of unsaturated carboxylic acids to reinforce NBR", *J. Appl. Polym. Sci*., **77**, 2740 (2000).
23. X. Yuan, Y. Zhang, Z. Peng, and Y. Zhang, "*In situ* preparation of magnesium methacrylate to reinforce NBR", *J. Appl. Polym. Sci*., **84**, 1403 (2002).
24. A. Du, Z. Peng, Y. Zhang, and Y. Zhang, "Polymerization conversion and structure of magnesium methacrylate in ethylene-vinyl acetate rubber vulcanizates", *J. Appl. Polym. Sci*., **93**, 2379 (2004).
25. T. Ikeda, S. Sakurai, K. Nakano, and B. Yamada, "Copolymerization of zinc methacrylate and perfluoroalkyl acrylate in hydrocarbon medium", *J. Appl. Polym. Sci*., **59**, 781 (1996).
26. T. Ikeda and B. Yamada, "Simulation of the *in situ* copolymerization of zinc methacrylate and 2-(*N*-ethylperfluoro-octanesulphonamido)ethyl acrylate in hydrogenated nitrile-butadiene rubber", *Polym. Int*., **48**, 367 (1999).
27. K. Horiuchi and A. Hamada, "Golf ball", *Europe Patent*, 0,582,487 A1, September 2, 1994.
28. D. S. Granatowicz, M. T. Morris, M. V. Pilkington, and G. R. Tompkin, "High modulus belt compostion and belts made therewith", *Europe Patent*, 0,864,607 A1, September 16, 1998.
29. Y. Keisaku, I. Kiyoshi, and K. Junichi, "Rubber composition", *Europe Patent*, 0,589,701 A1, March 30, 1994.
30. R. M. Freeman, W. L. Hergenrother, and F. J. Ravagnani, "High modulus low hysteresis rubber compound for pneumatic tires", *US Patent*, 5,464,899 A, November 7, 1995.
31. Z. M. Ariff, Z. Zakaria, L. H. Tay, and S. Y. Lee, "Effect of foaming temperature and rubber grades on properties of natural rubber foams", *J. Appl. Polym. Sci*., **107**, 2531 (2008).
32. J. H. Kim, K. C. Choi, J. M. Yoon, and S. Y. Kim, "Effects of Foaming temperature and carbon black content on the cure behaviors and foaming characteristics of the natural rubber foams", *Elastomer*, **41**, 147 (2006).
33. E. S. Park, "Mechanical properties and antibacterial activity of peroxide-cured silicone rubber foams", *J. Appl. Polym. Sci*., **110**, 1723 (2008).
34. G. Li and M. John, "A Crumb Rubber Modified Syntactic Foam", *Mater. Sci. Eng. A*, **474**, 390 (2008).
35. G. Li and N. Jones, "Development of Rubberized Syntactic Foam", *Composites Part A*, **38**, 1483 (2007).
36. R. Maharsia, N. Gupta, and H. D. Jerro, "Investigation of flexural strength properties of rubber and nanoclay reinforced hybrid syntactic foams", *Mater. Sci. Eng. A*, **417**, 249 (2006).
37. J. H. Kim, K. C. Choi, and J. M. Yoon, "The Foaming Characteristics and Physical Properties of Natural Rubber Foams: Effects of Carbon Black Content and Foaming Pressure", *J. Ind. Eng. Chem*., **12**, 795 (2006).
38. H. Jin, W. Y. Lu, S. Scheffel, M. K. Neilsen, and T. D. Hinnerichs, "Characterization of Mechanical Behavior of Polyurethane Foams using Digital Image Correlation", 2005 ASME International Mechanical Engineering Congress & Exposition, Nov. 5-11, Orlando, FL, USA.
39. Z. Xiao, R. Guan, Y. Jiang, and Y. Li, "Tensile property of thin microcellular PC sheets prepared by compression molding", *eXPRESS Polym. Lett*., **1**, 217 (2007).
40. S. M. Kang, S. J. Lee, and B. K. Kim, "Shape memory polyurethane foams", *eXPRESS Polym. Lett*., **6**, 63 (2012).
41. Z. Wang and T. J. Pinnavaia, "Nanolayer reinforcement of elastomeric polyurethane", *Chem. Mater*., **10**, 3769 (1998).
42. J. H. Chang and Y. U. An, "Nanocomposites of polyurethane with various organoclays: thermomechanical properties, morphology, and gas permeability", *J. Polym. Sci. Part B Polym. Phys*., **40**, 670 (2002).
43. Y. I. Tien and K. H. Wei, "High-tensile-property layered silicates/polyurethane nanocomposites by using reactive silicates as pseudo chain extenders", *Macromolecules*, **34**, 9045 (2001).
44. T. K. Chen, Y. I. Tien, and K. H. Wei, "Synthesis and characterization of novel segmented polyurethane/clay nanocomposites", *Polymer*, **41**, 1345 (2000).
45. X. Cao, L. J. Lee, T. Widya, and C. Macosko, "Polyurethane/clay nanocomposites foams: processing, structure and properties", *Polymer*, **46**, 775 (2005).
46. Y. Lu, L. Liu, D. Shen, C. Yang, and L. Zhang, "Infrared study on in situ polymerization of zinc dimethacrylate in poly

(α -octylene-*co*-ethylene) elastomer", *Polym. Int*., **53**, 802 (2004).
47. Z. Peng, X. Liang, Y. Zhang, and Y. Zhang, "Reinforcement of EPDM by *in situ* prepared zinc dimethacrylate", *J. Appl. Polym. Sci*., **84**, 1339 (2002).
48. H. D. Chae, U. Basuli, J. H. Lee, C. I. Lim, R. H. Lee, S. C. Kim, N. D. Jeon, and C. Nah, "Study on Mechanical and Thermal Properties of Rubber Composites Reinforced by Zinc Methacrylate and Carbon Black", *Polym. Compos*., 2012, DOI 10.1002/pc.22242.
49. S. Kaang, W. Jin, M. A. Kader, C. Nah, "Effects of blend composition and mixing method on mechanical and morphological properties of zinc dimethacrylate-reinforced acrylonitrile-butadiene copolymer nanocomposites.", *Polym. Plast. Technol*., **43**, 1517 (2004).
50. W. S. Kim, W. D. Kim, and S. I. Hong, "Fatigue life prediction of automotive rubber component subjected to a variable amplitude loading", *Elastomer*, **42**, 209 (2007).
51. C. Park and S. R. Nutt, "PM synthesis and properties of steel foams", *Mater. Sci. Eng. A*, **288**, 111 (2000).
52. T. Mukai, H. Kanahashi, T. Miyoshi, M. Mabuchi, T. G. Nieh, and K. Higashi, "Experimental study of energy absorption in a close-celled aluminum foam under dynamic loading", *Scripta Mater*., **40**, 921 (1999).
53. C. J. Yu, H. H. Eiferet, J. Banhart, and J. Baumeister, "Metal foams", *Adv. Mater. Processes*, **11**, 45 (1998).